HHS Public Access

Author manuscript

Neuroscience. Author manuscript; available in PMC 2016 September 10.

Published in final edited form as:

Neuroscience. 2015 September 10; 303: 323–337. doi:10.1016/j.neuroscience.2015.07.009.

Ultrastructural evidence for synaptic contacts between cortical noradrenergic afferents and endocannabinoid-synthesizing post-synaptic neurons

Beverly A. S. Reyes[1], **Nathan A. Heldt**[1], **Ken Mackie**[2], and **Elisabeth J. Van Bockstaele**[1]

[1]Department of Pharmacology and Physiology College of Medicine, Drexel University Philadelphia, PA 19102

[2]Psychological and Brain Sciences Indiana University Bloomington, IN 47405

Abstract

Endocannabinoids (eCBs) are involved in a myriad of physiological processes that are mediated through the activation of cannabinoid receptors, which are ubiquitously distributed within the nervous system. One neurochemical target at which cannabinoids interact to have global effects on behavior is brain noradrenergic circuitry. We, and others, have previously shown that CB type 1 receptors (CB1r) are positioned to pre-synaptically modulate norepinephrine (NE) release in the rat frontal cortex (FC). Diacylglycerol lipase (DGL) is a key enzyme in the biosynthesis of the endocannabinoid 2-arachidonoylglycerol (2-AG). While DGL-α is expressed in the FC in the rat brain, it is not known whether noradrenergic afferents target neurons expressing synthesizing enzymes for the endocannabinoid, 2-AG. In the present study, we employed high-resolution neuroanatomical approaches to better define cellular sites for interactions between noradrenergic afferents and FC neurons expressing DGL-α. Immunofluorescence microscopy showed close appositions between processes containing the norepinephrine transporter (NET) or dopamine-β-hydroxylase (DβH) and cortical neurons expressing DGL-α-immunoreactivity. Ultrastructural analysis using immunogold-silver labeling for DGL-α and immunoperoxidase labeling for NET or DβH confirmed that NET-labeled axon terminals were directly apposed to FC somata and dendritic processes that exhibited DGL-α-immunoreactivity. Finally, tissue sections were processed for immunohistochemical detection of DGL-α , CB1r and DβH. Triple label immunofluorescence revealed that CB1r and DβH were co-localized in common cellular profiles and these were in close association with DGL-α. Taken together, these data provide anatomical evidence for direct synaptic associations between noradrenergic afferents and cortical neurons exhibiting endocannabinoid synthesizing machinery.

Corresponding Author: Beverly A. S. Reyes, D.V.M., Ph.D., Department of Pharmacology and Physiology, College of Medicine, Drexel University, 245 S. 15th Street, Philadelphia, PA 19102, Voice: (215) 762-4932, Beverly.Reyes@drexelmed.edu.

Conflict of Interest

We declare no conflict of interest.

Keywords

cannabinoid receptor type 1; diacylglycerol lipase; norepinephrine transporter; dopamine-β-hydroxylase; electron microscopy

Introduction

The endogenous cannabinoids, or endocannabinoids (eCBs), are derived from phospholipids intrinsic to the plasma membrane and are one of the most ubiquitously distributed modulators in the central nervous system (Piomelli, 2003; Fride, 2005; Chevaleyre et al., 2006). The most abundant eCB in the mammalian brain is 2-arachidonoylglycerol (2-AG) (Mechoulam et al., 1995; Sugiura et al., 1995; Stella et al., 1997), which is synthesized in postsynaptic neurons by diacylglycerol lipase (DGL) (Bisogno et al., 2003) and degraded mainly by monoacylglycerol lipase (MGL) (Kitaura et al., 2001). Anatomical and physiological studies demonstrated and confirmed the critical involvement of eCBs in a variety of physiological and pathological processes including emotional reactivity, motivated behaviors and energy homeostasis (Hill et al., 2009; Bloomfield et al., 2014; Ceci et al., 2014; Hiebel et al., 2014; Romero-Zerbo and Bermudez-Silva, 2014). Endocannabinoids act on CB1r and CB2r, $G_{i/o}$ protein-coupled receptors with distinct distributions in the body (Castillo et al., 2012). Activation of CB1r most commonly results in the inhibition of neurotransmitter release (Castillo et al., 2012). CB2r are prevalent in the immune system and have been localized to microglia (Maresz et al., 2005; Bisogno and Di Marzo, 2010; Castillo et al., 2012).

The rate of eCB synthesis and degradation determines its signaling profile. Two primary mechanisms are known to be responsible for 2-AG synthesis: increases in intracellular Ca^{2+} via postsynaptic depolarization and activation of $G_{q/11}$ proteins leading to the activation of phospholipase **C (PLC)** via stimulation of several G protein-coupled receptors including group I metabotropic glutamate receptors, alpha 1 adrenergic receptors and some muscarinic receptors. PLC forms diacylglycerol from the hydrolysis of phosphatidylinositol, which DGL- then converts to 2-AG (Castillo et al., 2012). Biochemical analysis has shown that the DGL- isoform is the most abundant in brain (Bisogno et al., 2003; Gao et al., 2010; Tanimura et al., 2010) and DGL- immunoreactivity has been shown in several mammalian brain regions (Bisogno et al., 2003), including the pyramidal neurons of the FC (Lafourcade et al., 2007). The localization of DGL- in various brain regions also indicates putative interactions with other neurotransmitters/neuropeptides. Widespread function of CB1r modulation involves inhibition of neurotransmitter release (Freund et al., 2003; Chevaleyre et al., 2006; Garkun and Maffei 2014; Kury et al., 2014; Ramirez-Franco et al., 2014), while cannabinoid-induced neurotransmitter release has also been demonstrated in various brain regions (Tzavara et al., 2001; Tzavara et al., 2003; Oropeza et al., 2005; Muntoni et al., 2006; Page et al., 2008; Kirilly et al., 2013). Initially, the mechanism proposed for eCB release involved a depolarization-induced event followed by retrograde signaling and binding of the endogenous ligand to presynaptically distributed receptors (Piomelli, 2003; Chevaleyre et al., 2006; Castillo et al., 2012; Wang and Lupica, 2014).

Cannabinoids have been shown to interact with monoaminergic systems via the CB1r to have global effects on behavior. For example, CB1r antagonists enhance serotonergic neurotransmission (Gobbi et al., 2005; Le Foll et al., 2009) and CB1r activation can stimulate the release of norepinephrine (NE) and promote dopamine (DA) efflux in the cortex (Jentsch et al., 1997; Pistis et al., 2002; Oropeza et al., 2005; Page et al., 2007; Carvalho et al., 2010). One region in which cannabinoids exert important effects on behavior is the FC. The FC plays a crucial role in cognitive processes including executive functioning, decision making and recognition memory (Euston et al., 2012; Jahans-Price et al., 2014; Oksanen et al., 2014). Interactions between cannabinoid and noradrenergic systems in the FC have been demonstrated. Specifically, acute and repeated administration of a CB1r synthetic agonist is capable of increasing multiple indices of noradrenergic activity (Oropeza et al., 2007; Page et al., 2007; Page et al., 2008) including increasing cortical NE efflux and inducing alterations in expression levels of several adrenergic receptor subtypes in FC (Hillard and Bloom, 1982; Mendiguren and Pineda, 2006; Franklin and Carrasco, 2012; Franklin et al., 2013). We also demonstrated that pre-treatment with a CB1r agonist diminishes acute stress-induced noradrenergic transmission in the FC (Reyes et al., 2012a). Furthermore, we showed that stress sensitizes the cortical α2-AR response, making it resistant to desensitization by chronic activation of CB1rs (Reyes et al., 2012a). These findings reveal the stress-dependent nature of cannabinoid-adrenergic interactions. However, there remain gaps in our knowledge regarding how NE and eCBs interact in the FC. While DGL-α has been shown to be widely distributed throughout the brain (Bisogno et al., 2003; Katona et al., 2006; Yoshida et al., 2011; Nyilas et al., 2009), it is not known whether NE afferents in the FC are directly positioned to innervate cortical neurons that express DGL-α . . Here, we investigated cellular sites for interactions between NE and DGL-α in the FC using immunofluorescence and immunoelectron microscopy. Also, we demonstrate that CB1rs are localized to NE afferents that are pre-synaptically positioned to DGL-α containing cells in the FC.

Materials and Methods

The procedures used in the present study were approved by the Institutional Animal Care and Use Committee Drexel University and conformed to National Institute of Health's Guide for the Care and Use of Laboratory Animals. Rats were housed three per cage on a 12-h light schedule in a temperature controlled colony room (20 °C). They were allowed access to standard rat chow and water ad libitum and were acclimated to the housing facility for several days prior to handling. All efforts were made to utilize only the minimum number of animals necessary to produce reliable scientific data. Ten adult male Sprague-Dawley rats (Harlan Sprague-Dawley, Inc., Indianapolis, IN) weighing 225-250g and 7-8 weeks of age were used for immunofluorescence experiments to examine the cellular associations of DGL-α with norepinephrine transporter (NET) or the norepinephrine synthesizing enzyme, dopamine-beta-hydroxylase (DβH) in the FC. Seven rats were used for ultrastructural analysis of DGL-α and NET or DβH in the FC.

Specificity of antisera

The polyclonal DGL-α antibody was raised in rabbit against glutathione S-transferase fusion proteins containing residues 790-908 of human DGL-α as previously reported (Katona et al., 2006; Nyilas et al., 2009). The specificity of DGL-α antibody was previously established (Katona et al., 2006; Nyilas et al., 2009). In those studies, the specificity of DGL-α antibody was tested using HEK cells transiently expressing a V5 epitope-tagged DGL-α with either purified antibody or purified antibody preincubated with 5ug/mL immunizing protein (Katona et al. 2006). Purified antibody preincubated with immunizing protein strongly attenuated staining by the DGL-α antibody (Katona et al., 2006). Likewise, additional control experiments were conducted in the present study where the specificity of DGL-α was established by processing tissues sections from the FC in a cocktail of DGL-α and blocking peptide (1ug/mL) following pre-incubation at 4°C overnight. Pre-incubation with immunizing protein resulted in the absence of immunolabeling in tissues containing the FC.

The noradrenergic axon terminals were identified using either NET or DβH. The monoclonal antibody directed against the NET (MAb Technologies Inc.; Catalog number: NET05-1; Lot number: 220107) was generated using a peptide (amino acids 5-17) of a mouse and rat NET coupled to a keyhole limpet hemocyanin by addition of C-terminal cysteine. We previously established the specificity of NET antibody by preabsorption of the NET antibody with antigenic blocking peptide (1μg/mL; MAb Technologies Inc.). This experiment resulted in the absence of immunolabeling in rat tissues that were expected to show immunolabeling including nucleus accumbens, amygdala and FC (Carvalho et al., 2010; Kravets et al., 2013). The monoclonal antibody directed against purified bovine DβH was generated in mouse (Chemicon, Millipore, Billerica, MA; Catalog number: MAB 308; Lot number: NG1740906). We have previously demonstrated the specificity of DβH antibody (Oropeza et al., 2007). Additionally, validation by preabsorption with the antigenic blocking peptide (Alpha Diagnostics, San Antonio, TX) resulted in the absence of immunolabeling in tissue sections obtained from the FC. The CB1r, a polyclonal antibody directed towards the last 73 amino acid residues (401-473) of the rat CB1r was developed in rabbit (Suarez et al., 2008; Wager-Miller et al., 2002). We previously showed the specificity of CB1r using CB1r knock out mice in multiple brain regions to verify the lack of immunoreactivity in knockout animals (Scavone et al., 2010). Furthermore, the specificity of CB1r was also demonstrated using immunoblotting where a protein of the expected molecular size was detected (Suarez et al., 2008). In addition, we conducted an additional control experiments in the present study where the specificity of CB1r was established by processing tissues sections from the FC in a cocktail of CB1r and blocking peptide (2ug/mL) following preincubation at 4°C overnight. This procedure resulted in the absence of CB1r immunolabeling in the FC.

Moreover, specificity control for secondary antibodies was conducted by processing tissue sections without the primary antibody in parallel with the tissue sections incubated in primary antibody. Immunoperoxidase or immunogold-silver labeling was not detected in tissue sections from which primary antibody had been omitted. In order to evaluate potential cross-reactivity of secondary antibodies with the primary antisera, some tissue sections were

processed for dual immunolabeling experiments with omission of one of the primary antisera.

Immunofluorescence

The region analyzed using immunofluorescence and electron microscopy included primarily the infralimbic portion of the FC as represented in the rat brain atlas (Paxinos and Watson, 1997). At the level of bregma 2.20-3.20mm, the infralimbic region of the FC is bounded anteriorly by the medial orbital cortex, dorsally by the prelimbic cortex, laterally by the forceps minor of corpus callosum, as well as ventrally and caudally by the dorsal peduncular cortex and lateral septal nucleus.

Five rats were deeply anesthetized with sodium pentobarbital (80 mg/kg) intraperitoneally and transcardially perfused through the ascending aorta using 1) 20 ml heparinized saline and 2) 500 ml of 4% formaldehyde in 0.1 M phosphate buffer (PB; pH 7.4) by the Masterflex peristaltic pump (Cole-Parmer, Vernon Hills, IL) with the speed drive of 55 and 110 rpm for heparinized saline and formaldehyde, respectively. Brains were then removed and post fixed in 4% formaldehyde overnight at 4°C. Forty micrometer thick coronal sections through the FC were cut with a vibratome (Technical Product International, St Louis, MO, USA) and rinsed extensively in 0.1 M PB and 0.1 M tris-buffered saline (TBS; pH 7.6). An additional five rats were sacrificed for triple immunolabeling experiment. Sections were placed for 30 min in 1% sodium borohydride in 0.1 M PB to reduce amine-aldehyde compounds thereby diminishing autofluorescence (Clancy and Cauller, 1998). The tissue sections were then incubated in 0.5% bovine serum albumin (BSA) in 0.1M TBS for 30 min. Thorough rinses in 0.1 M TBS were done following incubation. Subsequently, sections were incubated in a cocktail containing rabbit anti-DGL-α at 1:000 and mouse anti-DβH (Chemicon International, Temecula, CA, USA) at 1:1,000 or mouse anti-NET (MAb Technologies Inc., Stone Mountain, GA) at 1:1,000 in 0.1% BSA and 0.25% Triton X-100 in 0.1M TBS. Some sections were also processed for triple immunolabeling with the addition of guinea pig anti-cannabinoid receptor type 1 (CB1; 1:2000). Incubation time was 15-18 h on a rotary shaker at room temperature. Sections were then washed in 0.1 M TBS and incubated in a secondary antibody cocktail containing fluorescein isothiocyanate (FITC) donkey anti-rabbit (1:200; Jackson ImmunoResearch Laboratories Inc., West Grove, PA, USA) and tetramethyl rhodamine isothiocyanate (TRITC) donkey anti-mouse (1:200; Jackson ImmunoResearch) antibodies prepared in 0.1 % BSA and 0.25% Triton X-100 in 0.1 M TBS for 2 h in the dark on a rotary shaker. For tissue sections processed for triple immunolabeling Alexa Fluor 647 donkey anti-guinea pig (1:200; Jackson ImmunoResearch) was added to a cocktail of secondary antibodies.

Following incubation with the secondary antibodies, the tissue sections were washed thoroughly in 0.1 M TBS. The tissue sections were then mounted on slides and allowed to dry in complete darkness. The slides were dehydrated in a series of alcohols, soaked in xylene and coverslipped using DPX (Sigma-Aldrich Inc., St. Louis, MO, USA). The tissue sections were then examined using a Olympus IX81 inverted microscope (Olympus, Hatagaya, Shibuya-Ku, Tokyo, Japan) equipped with lasers (Helium Neon laser and Argon laser; models GLG 7000; GLS 5414A and GLG 3135, Showa Optronics Co., Tokyo, Japan)

with the excitation wavelength of 488, 543 and 635. The microscope is also equipped with filters (DM 405-44; BA 505-605; and BA 560-660) and with Olympus Fluoview ASW FV1000 program (Olympus, Hatagaya, Shibuya-Ku, Tokyo, Japan). At least 8 tissue sections were taken from each of the five rats for dual labeling and 8 sections for triple labeling.

Electron microscopy

Seven rats were deeply anesthetized with sodium pentobarbital (80 mg/kg) and perfused transcardially through the ascending aorta with 10 ml heparinized saline followed with 50 ml of 3.75% acrolein (Electron Microscopy Sciences, Fort Washington, PA, USA) and 200 ml of 2% formaldehyde in 0.1 M PB (pH 7.4). The brains were removed immediately after perfusion fixation, sectioned into 1-3 mm coronal slices and postfixed with 2% formaldehyde in 0.1 M PB for 30 min and, if necessary, stored in 0.1 M PB for a short period prior to sectioning. The storage period was usually not more than 1-2 hours. Sections were cut in the coronal plane at a setting of 40 μm using a Vibratome (Technical Product International, St. Louis, MO) and collected into 0.1 M PB.

Forty-μm thick sections through the infralimbic area of the FC were processed for electron microscopic analysis of DGL-α and DβH or NET. Sections containing the FC were processed following the protocol described earlier for immunofluorescence except that Triton X- 100 was added at 0.01% to the solution for antibody incubation. Tissue sections were incubated in primary antibody cocktail containing rabbit anti-DGL-α at 1:000 and mouse anti-DβH (Chemicon International) at 1:1,000 or mouse anti-NET (Chemicon International) at 1:1,000 for 15-18 h at room temperature. The following day, tissue sections were rinsed three times in 0.1 M TBS and incubated in biotinylated donkey anti-rabbit (1:400; Vector Laboratories, Burlingame, CA, USA) for 30 min followed by rinses in 0.1 M TBS. Subsequently, a 30-minute incubation of avidin-biotin complex (Vector Laboratories) followed. For all incubations and washes, sections were continuously agitated with a rotary shaker. DGL-α was visualized by a 7-minute reaction in 22 mg of 3,3’-diaminobenzidine (Sigma-Aldrich Inc., St. Louis, MO) and 10 μl of 30% hydrogen peroxide in 100 ml of 0.1 M TBS.

Gold-silver localization of DβH or NET was carried out by rinsing the tissue sections three times with 0.1 M TBS, followed by rinses with 0.1 M PB and 0.01 M phosphate buffered saline (PBS; pH 7.4). Sections were then incubated in a 0.2% gelatin-PBS and 0.8% BSA buffer for 10 min. This was followed by incubation in goat anti-mouse IgG conjugate in 1 nm gold particles (Amersham Bioscience Corp., Piscataway, NJ, USA) at room temperature for 2 hours. Sections were then rinsed in buffer containing the same concentration of gelatin and BSA as above and subsequently rinsed with 0.01 M PBS. Sections were then incubated in 2% glutaraldehyde (Electron Microscopy Sciences) in 0.01 M PBS for 10 min followed by washes in 0.01 M PBS and 0.2 M sodium citrate buffer (pH 7.4). A silver enhancement kit (Amersham Bioscience Corp.) was used for silver intensification of the gold particles. The optimal times for silver enhancement were determined by empirical observation for each experiment and ranged 7-8 min. Following intensification, tissue sections were rinsed in 0.2 M citrate buffer and 0.1 M PB, and incubated in 2% osmium tetroxide (Electron

Microscopy Sciences) in 0.1 M PB for 1 h, washed in 0.1 M PB, dehydrated in an ascending series of ethanol followed by propylene oxide and flat embedded in Epon 812 (Electron Microscopy Sciences; (Leranth and Pickel, 1989). Ultrathin sections of approximately 70 nm were cut with a diamond knife (Diatome-US, Fort Washington, PA, USA) using a Leica Ultracut (Leica Microsystems). Sections were collected on copper mesh grids and counterstained with 5% aqueos uranyl acetate for 20 minutes followed by Reynold's lead citrate for 5-7minutes. Captured images of selected sections were compared with light microscopic images of the block face before sectioning to verify that the area of interest was targeted/collected. Sections were examined using a transmission electron microscope (TEM; Morgagni, Fei Company, Hillsboro,OR, USA) and digital images were captured using the AMT advantage HR/HR-B CCD camera system (Advance Microscopy Techniques Corp., Danvers, MA, USA). The TEM has an accelerating voltage of 80kv and we used the magnification of 11,000 to 14,000 in a field size of 9.3 μm × 9.3 μm for 11000× and 7.3 μm × 7.3 μm for 14000×. Figures were obtained in tiff files, assembled and adjusted for brightness and contrast in Adobe Photoshop.

Controls and Data analysis

Tissue sections for electron microscopy were taken from rats with the best immunohistochemical labeling and preservation of ultrastructural morphology. The semi-quantitative approach used in the present study is well established and has been described previously (Van Bockstaele et al., 1996a; Van Bockstaele et al., 1996b; Reyes et al., 2006; Reyes et al., 2007). While acrolein fixation optimizes the preservation of ultrastructural morphology, the caveat of limited and or differential penetration of immunoreagents in thick tissue sections exists (Leranth and Pickel, 1989; Chan et al., 1990). Consequently, the limited penetration of DGL- α, DβH and NET may result in an underestimation of the relative frequencies of their distribution. We mitigated this limitation by collecting the tissue sections exclusively near the tissue-Epon interface where penetration is maximal and profile were sampled only when all the markers were present in the surrounding neuropil included in the analysis The cellular elements were identified based on the description of Peters and colleagues (Peters and Palay, 1996). Somata contained a nucleus, Golgi apparatus and smooth endoplasmic reticulum. Proximal dendrites contained endoplasmic reticulum, were postsynaptic to axon terminals and were larger than 0.7 μm in diameter. A terminal was considered to form a synapse if it showed a junctional complex, a restricted zone of parallel membranes with slight enlargement of the intercellular space, and/or associated with postsynaptic thickening. A synaptic specialization was only limited to the profiles that form clear morphological characteristics of either Type I or Type II (Gray, 1959). Asymmetric synapses were identified by thick postsynaptic densities (Gray's type I; (Gray, 1959). In contrast, symmetric synapses had thin densities (Gray's type II; (Gray, 1959) both pre- and post-synaptically. An undefined synapse was defined as an axon terminal plasma membrane juxtaposed to that of a dendrite or soma devoid of recognizable membrane specializations and no intervening glial processes.

In sections dually labeled for DGL-α and DβH or NET, the number of DβH- or NET-labeled axon terminals was grouped from randomly selected ultrathin sections taken from four nonadjacent sections from each animal (n = 5). At least five sections were examined per

animal. From the surface of the individual epon block containing the tissue, at least four to eight ultrathin sections were collected. Fields of at least 11,000X magnification showing DβH or NET-labeled axon terminals, and DGL-α-labeled profiles were captured and classified. This approach resulted in 425 DGL-α-labeled profiles for tissue sections labeled for DβH and DGL-α and 407 DGL-α - labeled profiles for tissue sections labeled for NET and DGL-α. All potential neuronal targets of DβH or NET-labeled axon terminals throughout the analysis were examined by defining their total associations with other profiles regardless of whether a membrane specialization was seen within the plane of section. The postsynaptic targets considered included dendrites containing gold-silver labeling for DGL-α and dendrites lacking gold-silver labeling for DGL-α. DGL-α -labeled profiles forming clear synaptic specializations were classified as symmetric (Gray's Type II) or asymmetric (Gray's Type I). On the other hand, undefined contacts were characterized by a junctional complex that was not clearly distinguishable to allow a classification as either symmetric or asymmetric in the plane of section analyzed.

Identification of immunogold-silver labeling in profiles

Selective immunogold-silver labeled profiles were identified by the presence, in single thin sections, of at least two immunogold-silver particles within a cellular compartment. As we previously reported (Reyes, et al., 2006), single spurious immunogold-silver labeling can contribute to false positive labeling and can be detected on blood vessels, myeling or nuclei. ,Although minimal spurious labeling was identified in the present study, the criteria for defining a process as immunolabeled was therefore set at 2 immunogold-silver particles in a cellular profile. Whenever possible, the more lightly labeled somatic and dendritic labeling for DGL-α was confirmed by detection in at least two adjacent sections.

Results

Selection of markers for NE and control experiments

Control sections for dual and triple labeling immunofluorescence were processed in parallel where the primary or secondary antibodies were omitted in order to rule out any cross-reactivity. The following conditions were processed 1) primary antisera were omitted while secondary antibodies were added, 2) one of the primary antisera was omitted; 3) one of the secondary antibodies were omitted; and 4) all secondary antibodies were omitted. Tissue sections processed in the absence of primary or secondary antibody/ies did not exhibit detectable immunoreactivity/ies. Using confocal microscopy, there can be a concern regarding bleed through of signal in different channels. Settings were controlled so that individually labeled profiles could be detected in the sections analyzed (Figs. 1, 5).

We employed two different antibodies to visualize NE in the FC. One antibody recognized the noradrenergic synthesizing enzyme, DβH, and the other recognized the transporter protein responsible for reuptake of NE into noradrenergic axon terminals. DβH is a useful marker for noradrenergic terminals using light and fluorescence microscopy because of the ability to increase penetration with detergents in thicker tissue section. However, this vesicle-bound enzyme is sometimes more difficult to consistently detect using electron microscopy with low concentrations of permeabilization agents. To circumvent the potential

caveat of decreased detection of NE in axon terminals at the ulstrastructural level, we also examined the relationship of DGL with NET, which has been used effectively as a marker to detect noradrenergic axon terminals at the ultrastructural level (Carvalho et al., 2010; Kravets et al., 2013). Previous studies in our laboratory and others (Carvalho et al., 2010; Zhang et al., 2013) have shown an extensive dual localization of DβH and NET.

Control experiments processed in the absence of either DGL-α, NET or DβH antibody did not exhibit any detectable immunolabeling. We also evaluated the cross-reactivity of any of the primary antibodies (DGL-α, NET or DβH) with secondary antisera by processing tissue sections with the omission of one of each of the primary antisera. As we previously reported (Oropeza et al., 2007; Carvalho et al., 2010; Reyes et al., 2012a; Kravets et al., 2013), there was no detectable immunolabeling with the primary antibody omitted. Furthermore, processing of additional controls included incubation of each primary antibody with an inappropriate secondary antibody. This resulted in the absence of immunolabeling for the incorrectly paired primary-secondary antibody combination. Thus, control sections that were incubated with rabbit anti-DGL-α followed by goat anti-mouse secondary antibody did not exhibit any detectable DGL-α immunolabeling. Similarly, absence of immunolabeling was observed when control sections were incubated with mouse anti-NET followed by goat anti-rabbit secondary antibody. Control sections for electron microscopy were run in parallel in which one of the primary antisera was omitted but the rest of the processing procedure was identical. Sections processed in the absence of primary antibody did not exhibit immunoreactivity. To evaluate cross-reactivity of the primary antisera by secondary antisera, some sections were processed for dual labeling with omission of one of the primary antisera.

DGL-α and DβH or NET localization in the FC

Using fluorescence microscopy, DGL-α immunoreactivity could be visualized in the FC (Fig. 1B, 1E). DGL-α immunoreactivity exhibited a punctate-like appearance and appeared to define the contours of cells (Fig. 1B, 1E). Immunofluorescence labeling using two distinct fluorophore-tagged secondary antibodies to localize DGL-α and DβH or NET was conducted in the same section of tissue (Fig. 1A, 1D). Immunolabeling for DGL-α (green labeling; Fig. 1B, 1E) and DβH (red labeling; Fig. 1A) or NET (red labeling; Fig. 1D) were distributed in similar portions of the tissue section in the FC. Consistent with our previous report (Oropeza et al. 2007), DβH was localized to processes that were highly varicose and punctate in appearance (Figure 1A) while NET-labeled processes exhibited a simpler morphology (Figure 1D). Figure 1C and 1F indicate that DβH and NET-containing processes were in close association with cells expressing DGL-α . To further define substrates for putative interactions between DGL-α and DβH or NET, putative associations were further analyzed using immunoelectron microscopy.

Ultrastructural analysis of DGL-α and DβH or NET in the FC

Immunoperoxidase labeling for DβH/NET and immunogold-silver labeling for DGL-α , were localized in the same section of tissue in the area of interest sampled for semi-quantitative analysis (Figs. 2-4). The immunogold-silver deposits indicative of DGL-α were clearly distinguishable from the immunoperoxidase labeling indicative of DβH or NET

(Figs. 2-3). The region sampled in the FC for immunoelectron microscopy was the same as that shown for immunofluorescence microscopy (Figure 1B, 1E). Immunoperoxidase labeling for DβH and NET could be identified as an electron dense reaction product localized within vesicle-filled axon terminals (Figs. 2-4). The majority of the DβH and NET-containing profiles were unmyelinated axons and varicosities consistent with the previously reported localization of NET and DβH in the FC and other brain regions (Miner et al., 2003; Miner et al., 2006; Farb et al., 2010). The NET and DβH-immunoreactive axon terminals contained small clear vesicles (Figs. 2-4). While NET or DβH-immunolabeling was primarily localized in axon terminals, DGL-α immunoreactivity detected by immunogold-silver labeling was localized primarily in dendritic processes (Figs. 2-3) and somata (Figure 4). Immunogold-silver labeling for DGL-α appeared as irregular contoured black deposits that were distributed along the plasma membrane and within the cytoplasmic compartment of dendrites (Figs. 2-3). Semi-quantitative analysis showed that 59.93% (673/1123) of DGL-α-immunogold-silver particles in dendritic profiles were localized along the plasma membrane while 40.07% (450/1123) were distributed within the cytoplasmic compartment. Within somata, this difference was not as apparent as abundant immunoreactivity for DGL-α was localized to intracellular compartments (Fig. 4).

DβH or NET targets DGL-α in the FC

DGL-α, DβH or NET were abundant in the neuropil at the ultrastructural level (Figs. 2-4) where markers of NE (DβH or NET) were pre-synaptically distributed with respect to DGL-α-containing dendrites (Figs. 2B-C; Fig. 3), somata (Fig. 4) and unlabeled dendrites (Fig. 2A, 3A). Targets of NE axon terminals included small, large (Figs. 2; 3A, B-D) and longitudinal (not shown) dendritic processes. Semi-quantitative analysis revealed that of the 322 DβH-immunoreactive axon terminals observed in the neuropil, 23.91% (77/322) directly contacted dendrites exhibiting DGL-α-immunoreactivity. When synaptic complexes were identifiable between DβH-immunoreactive axon terminals and dendrites containing DGL-α, they were morphologically heterogeneous (Figs. 2, 3). Of the 77 DβH-immunoreactive axon terminals in direct contact with DGL-α-containing dendrites, 9.09% (7/77) formed asymmetric synapses while 58.44% (45/77) formed symmetric synapses (Fig. 2). The remainder of the DβH-immunoreactive axon terminals identified that contacted DGL-α-containing dendrites could not be unequivocally classified as asymmetric or symmetric and were classified as undefined. This is consistent with the known morphological features of monoaminergic axon terminals in the FC (Schroeter et al., 2000; Miner et al., 2003; Miner et al., 2006; Farb et al., 2010).

Of the 292 NET-immunoreactive axon terminals examined, 29.79% (82/292) formed direct contacts with DGL-α-containing dendrites (Fig. 3B-D). Of the 82 NET-immunoreactive axon terminals in contact with DGL-α-containing dendrites, 6.09% (5/82) formed asymmetric synapses while 62.20% (51/82) formed symmetric synapses (Fig. 3C). NET-immunoreactive axon terminals that formed asymmetric synapses were characterized by thick postsynaptic densities, while symmetric synapses had thin postsynaptic densities (Fig. 3C). Many NET-immunoreactive axon terminals formed undefined synapses with DGL-α-containing dendrites (Figs. 3B, D). About 31.71% (26/82) of the NET-containing axon terminals formed undefined synapses with DGL-α-containing dendrites. Of the 387 DGL-α-

immunoreactive dendrites, 25.47% (82 DGL-α-immunolabeled dendrites/332 NET-immunolabeled axon terminals) were targeted by NET. Of the 387 DGL-α-immunoreactive dendrites, 19.89% (77 DGL-α--immunolabeled dendrites /387 DβH-immunolabeled axon terminals) were targeted by DβH.

DGL-α, CB1r and DβH or NET localization in the FC

Triple label immunofluorescence was conducted in the same tissue sections through the FC where DGL-α was labeled with FITC, CB1r was labeled with TRITC and DβH was labeled with Alexa Fluor 647 (Fig. 5A-D). Fibers exhibiting immunolabeling for CB1r (red labeling) were co-localized with DβH (blue labeling), consistent with our previous anatomical investigation (Oropeza et al., 2007). When co-localization with CB1r and DβH was observed, they were distributed in close association with DGL-α (Fig. 5D).

Discussion

Results from the high-resolution anatomical studies presented here indicate that cortical noradrenergic fibers are in direct contact with neurons that contain the molecular machinery to release eCBs. This is the first direct anatomical evidence indicating a basis for an interaction between cortical noradrenergic afferents and eCB-synthesizing neurons. Taken with the triple immunofluorescence studies provided showing close associations between NE afferents containing CB1r and eCB-synthesizing cortical neurons, the present findings suggest that release of eCBs from cortical neurons may pre-synaptically regulate NE release via CB1r activation.

Methodological considerations

Investigation of synaptic associations using immunohistochemical detection of an antibody combined with electron microscopy offers some advantages. For instance, the pre-embedding immunohistochemical technique maintains morphological preservation of discreet subcellular localization of the antigen of interest. The dual immunolabeling procedure where immunoperoxidase detection is combined with immunogold-silver detection permits identifying synaptic specialization within the defined neuronal populations. Nevertheless, there are also some caveats inherent to this experimental approach. In order to overcome the limitations associated with the specificity of immunogold-silver labeling, we only quantified profiles containing two or more immunogold-silver particles. This approach may result to an underestimation of the actual synaptic associations; however, this minimized the inclusion of potential spurious immunogold-silver labeling. Since DβH is a vesicular-bound enzyme, detection becomes more difficult without using enhancement methods such as using detergents e.g. Triton X-100. However, the use of permeabilization agents compromises the integrity of the ultrastructure preservation. In order to circumvent this caveat, we use a very small amount of Triton X-100 at 0.01% following the procedures reported by Farb and colleagues (Farb et al., 2010). Additionally, we also used an antibody directed against NET as an additional marker of noradrenergic axon terminals that is more readily detectable using electron microscopic analysis (Kravetz et al., 2013; Erickson et al., 2011).

Our data are consistent with previous descriptions of the morphological differentiation of noradrenergic terminals (Miner et al., 2003; Miner et al., 2006; Farb et al., 2010). These characteristics include the following: 1) the preponderance of immunoreactivity in axons that lack myelin, 2) small vesicle content within the cytoplasm, and 3) the occurrence of dense core vesicles in some profiles. Although our data are consistent with previous studies, an underestimation of the identity of synaptic specializations may have occurred. Factors that might account for this underestimation are 1) lack of detergent used to permeabilize membranes for improving antibody penetration and 2) a high density of immunoperoxidase reaction product causing the defined feature of labeled axon terminals to be ambiguous.

DGL-α is post-synaptic to NE afferents in the FC

Our findings on DGL-α localization are consistent with reports examining other brain areas including the basolateral amygdala and dorsal horn showing a predominantly post-synaptic distribution of DGL-α (Nyilas et al., 2009; Yoshida et al., 2011;). The preponderance of DGL-α at the postsynaptic site is consistent with the widely accepted notion that 2-AG is synthesized in the postsynaptic neuron and through retrograde signaling binds to CB1r distributed in the noradrenergic-containing axon terminals in the FC (Oropeza et al., 2007). Previous studies have shown that DGL-α is localized along the plasma membrane in striatum (Uchigashima et al., 2007) and ventromedial nucleus of the hypothalamus (Reguero et al., 2014). In the present study, the localization of DGL-α along the plasma membrane may suggest that 2-AG could rapidly leave the cell following synthesis.

The present data are also consistent with other reports, albeit in mice, showing the localization of key proteins involved in eCB signaling in layers V/VI of the mouse prelimbic area of the FC (Lafourcade et al., 2007). Using immunoelectron microscopy, LaFourcade and colleagues (2007) identified DGL-α in cortical dendritic processes that were postsynaptic to afferents containing CB1r and further demonstrated that DGL-α co-localizes with the excitatory amino acid receptor, mGluR5. The present study builds on these results by providing the first demonstration that NE afferents exhibiting CB1r are pre-synaptic to neurons expressing synthetic enzymes for eCB synthesis.

Synaptic specializations of DβH/NET afferents with DGL-α neurons are heterogeneous—Although the present results show that majority of the NET and DβH-immunoreactive axon terminals do not form classically defined synaptic contacts, a finding that is in agreement with previous electron microscopic studies (Schroeter et al., 2000; Miner et al. 2003; Miner et al. 2006; Farb et al. 2010), our results show a slightly higher percentage of synapses formed by NET- and DβH-immunoreactive axon terminals with DGL-α -immunoreactive dendrites compared to previous reports on synapses formed by NE afferents in the FC (Miner et al., 2003; Miner et al., 2006; Farb et al., 2010). Previously, 24% (37/157: Miner et al., 2003) and 18% (130/736: Miner et al., 2006) of NET-immunoreactive terminals and 18% (75/410) of DβH-immunoreactive axon terminals (Farb et al., 2010) form synapses in the prelimbic area of the prefrontal cortex. This difference may be due to regional differences in the FC investigated across studies. Furthermore, it is also possible that a dense immunoperoxidase reaction product obscured clear identification of synapses. When synapses were identifiable between NE afferents and DGL-α-

immunoreactive targets, they possessed junctions that were characteristic of inhibitory transmission. Consistent with other reports (Miner et al., 2003; Miner et al., 2006), NET axon terminals examined here exhibited predominantly symmetric type synaptic specializations in the FC. Similarly, DβH axon terminals have been shown to form a greater number of symmetric as compared to asymmetric synapses in other brain regions (Farb et al., 2010), consistent with the findings reported here. Symmetric synapses are believed to mediate inhibition and have been correlated with gamma-aminobutyric acid (GABA) transmission (Peters et al., 1991; Peters and Palay, 1996). Axon terminals labeled with the inhibitory transmitter GABA have been shown to exhibit symmetric synapses in multiple regions of the brain (Carlin et al., 1980; Omelchenko and Sesack, 2009) including the FC (Carr and Sesack, 2000). Moreover, we and others have shown the presence of CB1rs on NE afferents (Oropeza et al., 2007; Eggan et al., 2010; Richter et al., 2012). Taken together, the morphological characteristics of the synapses formed by NET and DβH axon terminals suggest that they may localize within an inhibitory afferent such as GABA but further studies are required to unequivocally establish this possibility (Fig. 6). In such a scenario, following DGL-α action on eCB synthesis, 2-AG may diffuse into the synapse and may effectively suppress GABA release. Retrograde suppression of GABA release will profoundly influence neural activity and release of neuromodulators, which may then affect synaptic integration and plasticity of post-synaptic processes. For instance, prolonged stimulation using a cannabinoid agonist, HU-210 in cerebellar granule cells induces silencing of CB1r and mutes GABA-containing axon terminals (Ramirez-Franco et al., 2014). To unequivocally establish such a cellular interaction, a triple immunolabeling using immunoperoxidase and dual immunogold labeling approach (Reyes et al., 2011; Reyes et al., 2012b; Kravets et al., 2013) may be carried out in future studies.

In the present study, a small percentage of NET and DβH axon terminals formed asymmetric synapses. Asymmetric synapses are believed to mediate excitation based largely on the detection of thickened postsynaptic densities in regions of the brain containing higher proportions of excitatory synapses (Carlin et al., 1980). The asymmetric architecture formed by NET and DβH may reflect co-localization with glutamate, which is known to be excitatory in FC and form asymmetric-type synapses (Katona et al., 2006). In the rat spinal cord, it has been shown that DGL-α was localized post-synaptically in cellular profiles that receive asymmetric synapses from axon terminals containing CB1r (Nyilas et al., 2009). Using a combination of genetic and targeted lipidomic approaches, DGL-α mediates group 1 glutamate receptor-induced mobilization of 2-AG and this action requires interaction of DGL-α with coiled-coil-Homer proteins Homer-1b and Homer-2 (Jung et al., 2007). The localization of CB1r in axon terminals is strategically positioned to bind 2-AG and thus adjust presynaptic glutamate release. In the present study, it is tempting to speculate that NE afferents are also excitatory (e.g. afferents containing glutamate) and may be regulated by eCBs released from postsynaptic neurons via actions on pre-synaptically distributed CB1rs (Figure 6). Future studies are needed to define the frequency of co-localization of NET/DβH and glutamate in axon terminals and whether these terminals contact DGL-α in the FC. We have developed a triple immunoelectron microscopy approach that will help unveil this potential subcellular interaction in future studies (Reyes et al., 2011; Reyes et al., 2012b; Kravets et al., 2013).

Functional implications of eCB-regulation of cortical noradrenergic afferents—Recognition of the involvement of the eCB system in the regulation of mood, and specifically its role in depression and anxiety arose, in part, from clinical studies (Parolaro et al., 2010; Hauer et al., 2014). A significant increase in CB1r density and efficacy was reported in the dorsolateral FC of depressed suicide victims, suggesting that altered functioning of the eCB system in the FC could contribute to depression (Hungund et al., 2004; Parolaro et al., 2010). Known to be modulated by a number of neurochemically distinct neural pathways, the FC receives multiple afferent projections, one of which arises from the locus coeruleus (LC) (Dahlstroem and Fuxe, 1964; Berridge and Waterhouse, 2003; Chandler et al., 2014), a nucleus in the dorsal pontine tegmentum that contains the largest cluster of brain noradrenergic neurons. The release of NE is related to arousal states and this in turn has profound effects on cognitive, executive and behavioral processes (Lapiz and Morilak, 2006; Arnsten, 2007). Considering that NE is a key regulator of FC function, either too little or too much adrenergic neurotransmission results in suboptimal neuronal responses to exteroceptive or interoceptive stimuli (Berridge and Waterhouse, 2003; Devilbiss et al., 2012). High levels of noradrenergic transmission are implicated in behavioral, cognitive, emotional and physiological manifestations characteristic of depression and anxiety (Miller et al., 1996; Sands et al., 2000; Cottingham and Wang, 2012). We and others have demonstrated the presence of CB1rs on NE afferents (Oropeza et al., 2007; Eggan et al., 2010; Richter et al., 2012). Furthermore, CB1r mRNA has been detected in catecholaminergic and monoaminergic perikarya of the LC (Matsuda et al., 1993; Tsou et al., 1998). Exposure to WIN 55,212-2, a CB1r agonist, significantly increases NE efflux in the FC following both acute and chronic exposure (Oropeza et al., 2005; Page et al., 2007) and this is accompanied by increased anxiety-like behaviors (Page et al., 2007). Likewise, direct local infusion of WIN 55,212-2 into the FC increases cortical NE efflux (Page et al., 2008). However, electrophysiological studies have shown that acute and chronic treatment with WIN 55,212-2 blocked increases in layer V/VI cortical pyramidal cell excitability and increases in input resistance evoked by the α2-adrenergic receptor (α2-ARs) agonist, clonidine, indicating a desensitization of α2-ARs (Cathel et al., 2014).

Two primary mechanisms are known to be responsible for 2-AG synthesis: increases in intracellular Ca^{2+} via postsynaptic depolarization and activation of Gq/11 proteins, leading to PLC production via stimulation of group I metabotropic glutamate receptors. Figure 6 provides a schematic illustration of proposed mechanisms whereby eCB production can affect cortical NE afferents. Since the alpha1 adrenergic receptor primarily signals through Gq/11 proteins (Sawaki et al., 1995; Docherty, 1998; Chen and Minneman, 2005) its activation can stimulate eCB production to cause inhibition of NE efflux. Activation of alpha1 adrenergic receptors has been shown to lead to paracrine transactivation of CB1r (Turu and Hunyady, 2010; Gyombolai et al., 2012). Generally, protein kinase A is inhibitory on PLC (Tawfeek et al., 2008); however, when NE is released, the possibility exists that NE could augment responses by beta adrenergic receptor stimulation of voltage-gated calcium channels as it has been recently shown that NE upregulates voltage-gated calcium channel (Yu et al., 2015). This would then increase calcium influx during depolarization and consequently resulting in more 2-AG production (Figure 6). Although this is an interesting possibility, to our knowledge this mechanism has not yet been elucidated. Finally, the

potential exists that other GPCRs that do not signal through these mechanisms but markedly affect depolarization, are involved in altering eCB synthesis and subsequently CB1r activation of NE afferents.

The results of the present study extend our knowledge of eCB localization and noradrenergic afferents in the FC. It is tempting to speculate that the eCB system via release from cortical neurons may regulate NE afferents by acting on pre-synaptically distributed CB1rs. Dysregulation of FC neuronal activity and resultant effects on the NE system may contribute to the pathophysiology of FC-related psychiatric disorders. Both neuronal activation and neurotransmitter release depend on local production of eCBs and thus, local eCB concentrations may be crucial in the net effect of NE in cortical networks. In summary, the present study reveals that components of eCB synthesis may serve as a target in developing new therapeutic opportunities for the treatment of anxiety and depression disorders involving noradrenergic circuitry.

Acknowledgments

This project was supported by the National Institutes of Health grant DA #020129 to E.V.B.

References

Arnsten AF. Catecholamine and second messenger influences on prefrontal cortical networks of “representational knowledge”: a rational bridge between genetics and the symptoms of mental illness. Cereb Cortex. 2007; 17(Suppl 1):i6–i15. [PubMed: 17434919]

Berridge CW, Waterhouse BD. The locus coeruleus-noradrenergic system: modulation of behavioral state and state-dependent cognitive processes. Brain Res Brain Rev. 2003; 42:33–84.

Bisogno T, Di Marzo V. Cannabinoid receptors and endocannabinoids: role in neuroinflammatory and neurodegenerative disorders. CNS Neurol Disord Drug Targets. 2010; 9:564–573. [PubMed: 20632970]

Bisogno T, Howell F, Williams G, Minassi A, Cascio MG, Ligresti A, Matias I, Schiano-Moriello A, Paul P, Williams EJ, Gangadharan U, Hobbs C, Di Marzo V, Doherty P. Cloning of the first sn1-DAG lipases points to the spatial and temporal regulation of endocannabinoid signaling in the brain. J Cell Biol. 2003; 163:463–468. [PubMed: 14610053]

Blankman JL, Simon GM, Cravatt BF. A comprehensive profile of brain enzymes that hydrolyze the endocannabinoid 2-arachidonoylglycerol. Chem Biology. 2007; 14:1347–1356.

Bloomfield MA, Morgan CJ, Kapur S, Curran HV, Howes OD. The link between dopamine function and apathy in cannabis users: an [18F]-DOPA PET imaging study. Psychopharmacology (Berl). 2014; 231:2251–2259. [PubMed: 24696078]

Burette AC, Weinberg RJ, Sassani P, Abuladze N, Kao L, Kurtz I. The sodium-driven chloride/bicarbonate exchanger in presynaptic terminals. J Comp Neurol. 2012; 520:1481–1492. [PubMed: 22102085]

Carlin RK, Grab DJ, Cohen RS, Siekevitz P. Isolation and characterization of postsynaptic densities from various brain regions: enrichment of different types of postsynaptic densities. J Cell Biol. 1980; 86:831–845. [PubMed: 7410481]

Carr DB, Sesack SR. GABA-containing neurons in the rat ventral tegmental area project to the prefrontal cortex. Synapse. 2000; 38:114–123. [PubMed: 11018785]

Carvalho AF, Mackie K, Van Bockstaele EJ. Cannabinoid modulation of limbic forebrain noradrenergic circuitry. Eur J Neurosci. 2010; 31:286–301. [PubMed: 20074224]

Castillo PE, Younts TJ, Chavez AE, Hashimotodani Y. Endocannabinoid signaling and synaptic function. Neuron. 2012; 76:70–81. [PubMed: 23040807]

Cathel AM, Reyes BA, Wang Q, Palma J, Mackie K, Van Bockstaele EJ, Kirby LG. Cannabinoid modulation of alpha2 adrenergic receptor function in rodent medial prefrontal cortex. Eur J Neurosci. 2014; 40:3202–3214. [PubMed: 25131562]

Ceci C, Mela V, Macri S, Marco EM, Viveros MP, Laviola G. Prenatal corticosterone and adolescent URB597 administration modulate emotionality and CB1 receptor expression in mice. Psychopharmacology (Berl). 2014; 231:2131–2144. [PubMed: 24311359]

Chan J, Aoki C, Pickel VM. Optimization of differential immunogold-silver and peroxidase labeling with maintenance of ultrastructure in brain sections before plastic embedding. J Neurosci Methods. 1990; 33:113–127. [PubMed: 1977960]

Chandler DJ, Gao WJ, Waterhouse BD. Heterogeneous organization of the locus coeruleus projections to prefrontal and motor cortices. Proc Natl Acad Sci U S A. 2014; 111:6816–6821. [PubMed: 24753596]

Chen ZJ, Minneman KP. Recent progress in alpha1-adrenergic receptor research. Acta Pharmacologica Sinica. 2005; 26:1281–1287. [PubMed: 16225747]

Chevaleyre V, Takahashi KA, Castillo PE. Endocannabinoid-mediated synaptic plasticity in the CNS. Annu Rev Neurosci. 2006; 29:37–76. [PubMed: 16776579]

Cottingham C, Wang Q. Alpha2 adrenergic receptor dysregulation in depressive disorders: implications for the neurobiology of depression and antidepressant therapy. Neurosci Biobehav Rev. 2012; 36:2214–2225. [PubMed: 22910678]

Dahlstroem A, Fuxe K. Evidence for the Existence of Monoamine-Containing Neurons in the Central Nervous System. I. Demonstration of Monoamines in the Cell Bodies of Brain Stem Neurons. Acta Physiologica Scandinavica Supplementum Suppl. 1964; 232:231–255.

Devilbiss DM, Waterhouse BD, Berridge CW, Valentino R. Corticotropin-releasing factor acting at the locus coeruleus disrupts thalamic and cortical sensory-evoked responses. Neuropsychopharmacology. 2012; 37:2020–2030. [PubMed: 22510725]

Di Marzo V, Ligresti A, Morera E, Nalli M, Ortar G. The anandamide membrane transporter. Structure-activity relationships of anandamide and oleoylethanolamine analogs with phenyl rings in the polar head group region. Bioorganic Medicinal Chem. 2004; 12:5161–5169.

Docherty JR. Subtypes of functional alpha1- and alpha2-adrenoceptors. Eur J Pharmacol. 1998; 361:1–15. [PubMed: 9851536]

Eggan SM, Melchitzky DS, Sesack SR, Fish KN, Lewis DA. Relationship of cannabinoid CB1 receptor and cholecystokinin immunoreactivity in monkey dorsolateral prefrontal cortex. Neuroscience. 2010; 169:1651–1661. [PubMed: 20542094]

Enomoto T, Tse MT, Floresco SB. Reducing prefrontal gamma-aminobutyric acid activity induces cognitive, behavioral, and dopaminergic abnormalities that resemble schizophrenia. Biol Psychiatry. 2011; 69:432–441. [PubMed: 21146155]

Erickson SL, Gandhi AR, Asafu-Adjei JK, Sampson AR, Miner L, Blakely RD, Sesack SR. Chronic desipramine treatment alters tyrosine hydroxylase but not norepinephrine transporter immunoreactivity in norepinephrine axons in the rat prefrontal cortex. Int J Neuropsychopharmacol. 2011; 14:1219–1232. [PubMed: 21208501]

Euston DR, Gruber AJ, McNaughton BL. The role of medial prefrontal cortex in memory and decision making. Neuron. 2012; 76:1057–1070. [PubMed: 23259943]

Farb CR, Chang W, Ledoux JE. Ultrastructural characterization of noradrenergic axons and Beta-adrenergic receptors in the lateral nucleus of the amygdala. Front Behav Neurosci. 2010; 4:162. [PubMed: 21048893]

Franklin JM, Carrasco GA. Cannabinoid-induced enhanced interaction and protein levels of serotonin 5-HT(2A) and dopamine D(2) receptors in rat prefrontal cortex. J Psychopharmacol. 2012; 26:1333–1347. [PubMed: 22791651]

Franklin JM, Mathew M, Carrasco GA. Cannabinoid-induced upregulation of serotonin 2A receptors in the hypothalamic paraventricular nucleus and anxiety-like behaviors in rats. Neurosci Lett. 2013; 548:165–169. [PubMed: 23721787]

Freund TF, Katona I, Piomelli D. Role of endogenous cannabinoids in synaptic signaling. Physiol Rev. 2003; 83:1017–1066. [PubMed: 12843414]

Fride E. Endocannabinoids in the central nervous system: from neuronal networks to behavior. Curr Drug Targets CNS Neurol Disord. 2005; 4:633–642. [PubMed: 16375681]

Gao Y, Vasilyev DV, Goncalves MB, Howell FV, Hobbs C, Reisenberg M, Shen R, Zhang MY, Strassle BW, Lu P, Mark L, Piesla MJ, Deng K, Kouranova EV, Ring RH, Whiteside GT, Bates B, Walsh FS, Williams G, Pangalos MN, Samad TA, Doherty P. Loss of retrograde endocannabinoid signaling and reduced adult neurogenesis in diacylglycerol lipase knock-out mice. J Neurosci. 2010; 30:2017–2024. [PubMed: 20147530]

Garkun Y, Maffei A. Cannabinoid-dependent potentiation of inhibition at eye opening in mouse V1. Front Cell Neurosci. 2014; 8:46. [PubMed: 24600349]

Gobbi G, Bambico FR, Mangieri R, Bortolato M, Campolongo P, Solinas M, Cassano T, Morgese MG, Debonnel G, Duranti A, Tontini A, Tarzia G, Mor M, Trezza V, Goldberg SR, Cuomo V, Piomelli D. Antidepressant-like activity and modulation of brain monoaminergic transmission by blockade of anandamide hydrolysis. Proc Natl Acad Sci U S A. 2005; 102:18620–18625. [PubMed: 16352709]

Gray EG. Axosomatic and axo-dendritic synapses of the cerebral cortex: an electron microscopic study. J Anat. 1959; 93:420–433. [PubMed: 13829103]

Gyombolai P, Pap D, Turu G, Catt KJ, Bagdy G, Hunyady L. Regulation of endocannabinoid release by G proteins: a paracrine mechanism of G protein-coupled receptor action. Mol Cell Endocrinol. 2012; 353:29–36. [PubMed: 22075205]

Hajos N, Katona I, Naiem SS, MacKie K, Ledent C, Mody I, Freund TF. Cannabinoids inhibit hippocampal GABAergic transmission and network oscillations. Eur J Neurosci. 2000; 12:3239–3249. [PubMed: 10998107]

Hauer D, Kaufmann I, Strewe C, Briegel I, Campolongo P, Schelling G. The role of glucocorticoids, catecholamines and endocannabinoids in the development of traumatic memories and posttraumatic stress symptoms in survivors of critical illness. Neurobiol Learn Mem. 2014; 112:68–74. [PubMed: 24125890]

Hauer D, Schelling G, Gola H, Campolongo P, Morath J, Roozendaal B, Hamuni G, Karabatsiakis A, Atsak P, Vogeser M, Kolassa IT. Plasma concentrations of endocannabinoids and related primary fatty acid amides in patients with post-traumatic stress disorder. PLoS One. 2013; 8:e62741. [PubMed: 23667516]

Hiebel C, Kromm T, Stark M, Behl C. Cannabinoid receptor 1 modulates the autophagic flux independent of mTOR- and BECLIN1-complex. J Neurochem. 2014; 131:484–497. [PubMed: 25066892]

Hill MN, Hillard CJ, Bambico FR, Patel S, Gorzalka BB, Gobbi G. The therapeutic potential of the endocannabinoid system for the development of a novel class of antidepressants. Trends Pharmacol Sci. 2009; 30:484–493. [PubMed: 19732971]

Hillard CJ, Bloom AS. Delta 9-Tetrahydrocannabinol-induced changes in beta-adrenergic receptor binding in mouse cerebral cortex. Brain Res. 1982; 235:370–377. [PubMed: 6329417]

Hungund BL, Vinod KY, Kassir SA, Basavarajappa BS, Yalamanchili R, Cooper TB, Mann JJ, Arango V. Upregulation of CB1 receptors and agonist-stimulated [35S]GTPgammaS binding in the prefrontal cortex of depressed suicide victims. Mol Psychiatry. 2004; 9:184–190. [PubMed: 14966476]

Jahans-Price T, Gorochowski TE, Wilson MA, Jones MW, Bogacz R. Computational modeling and analysis of hippocampal-prefrontal information coding during a spatial decision-making task. Front Behav Neurosci. 2014; 8:62. [PubMed: 24624066]

Jentsch JD, Andrusiak E, Tran A, Bowers MB Jr, Roth RH. Delta 9-tetrahydrocannabinol increases prefrontal cortical catecholaminergic utilization and impairs spatial working memory in the rat: blockade of dopaminergic effects with HA966. Neuropsychopharmacology. 1997; 16:426–432. [PubMed: 9165498]

Jung KM, Astarita G, Zhu C, Wallace M, Mackie K, Piomelli D. A key role for diacylglycerol lipase-alpha in metabotropic glutamate receptor-dependent endocannabinoid mobilization. Mol Pharmacol. 2007; 72:612–621. [PubMed: 17584991]

Katona I, Urban GM, Wallace M, Ledent C, Jung KM, Piomelli D, Mackie K, Freund TF. Molecular composition of the endocannabinoid system at glutamatergic synapses. J Neurosci. 2006; 26:5628–5637. [PubMed: 16723519]

Kawamura Y, Fukaya M, Maejima T, Yoshida T, Miura E, Watanabe M, Ohno-Shosaku T, Kano M. The CB1 cannabinoid receptor is the major cannabinoid receptor at excitatory presynaptic sites in the hippocampus and cerebellum. J Neurosci. 2006; 26:2991–3001. [PubMed: 16540577]

Kirilly E, Hunyady L, Bagdy G. Opposing local effects of endocannabinoids on the activity of noradrenergic neurons and release of noradrenaline: relevance for their role in depression and in the actions of CB(1) receptor antagonists. J Neural Transm. 2013; 120:177–186. [PubMed: 22990678]

Kitaura S, Suzuki K, Imamura S. Monoacylglycerol lipase from moderately thermophilic Bacillus sp. strain H-257: molecular cloning, sequencing, and expression in Escherichia coli of the gene. J Biochem. 2001; 129:397–402. [PubMed: 11226879]

Kravets JL, Reyes BAS, Unterwald EM, Van Bockstaele EJ. Direct targeting of peptidergic amygdalar neurons by noradrenergic afferents: linking stress-integrative circuitry. Brain Struct Funct. 2013; 220:541–548. [PubMed: 24271021]

Kury LT, Yang KH, Thayyullathil FT, Rajesh M, Ali RM, Shuba YM, Howarth FC, Galadari S, Oz M. Effects of endogenous cannabinoid anandamide on cardiac Na/Ca exchanger. Cell Calcium. 2014; 55:231–237. [PubMed: 24674601]

Lafourcade M, Elezgarai I, Mato S, Bakiri Y, Grandes P, Manzoni OJ. Molecular components and functions of the endocannabinoid system in mouse prefrontal cortex. PLoS One. 2007; 2:e709. [PubMed: 17684555]

Lapiz MD, Morilak DA. Noradrenergic modulation of cognitive function in rat medial prefrontal cortex as measured by attentional set shifting capability. Neuroscience. 2006; 137:1039–1049. [PubMed: 16298081]

Le Foll B, Gorelick DA, Goldberg SR. The future of endocannabinoid-oriented clinical research after CB1 antagonists. Psychopharmacology (Berl). 2009; 205:171–174. [PubMed: 19300982]

Leranth, C.; Pickel, VM. Electron microscopic preembedding double-labeling methods.. In: Heimer, L.; Zaborszky, L., editors. Neuroanatomical tracing methods 2. 1st Ed.. Plenum Press; New York: 1989. p. 129-172.

Mackie K, Devane WA, Hille B. Anandamide, an endogenous cannabinoid, inhibits calcium currents as a partial agonist in N18 neuroblastoma cells. Mol Pharmacol. 1993; 44:498–503. [PubMed: 8371711]

Maresz K, Carrier EJ, Ponomarev ED, Hillard CJ, Dittel BN. Modulation of the cannabinoid CB2 receptor in microglial cells in response to inflammatory stimuli. J Neurochem. 2005; 95:437–445. [PubMed: 16086683]

Matsuda LA, Bonner TI, Lolait SJ. Localization of cannabinoid receptor mRNA in rat brain. J Comp Neurol. 1993; 327:535–550. [PubMed: 8440779]

Mechoulam R, Ben-Shabat S, Hanus L, Ligumsky M, Kaminski NE, Schatz AR, Gopher A, Almog S, Martin BR, Compton DR, Pertwee RG, Griffin G, Bayewitch M, Barg J, Vogel Z. Identification of an endogenous 2-monoglyceride, present in canine gut, that binds to cannabinoid receptors. Biochem Pharmacol. 1995; 50:83–90. [PubMed: 7605349]

Mendiguren A, Pineda J. Systemic effect of cannabinoids on the spontaneous firing rate of locus coeruleus neurons in rats. Eur J Pharmacol. 2006; 534:83–88. [PubMed: 16483566]

Miller HL, Delgado PL, Salomon RM, Berman R, Krystal JH, Heninger GR, Charney DS. Clinical and biochemical effects of catecholamine depletion on antidepressant-induced remission of depression. Arch Gen Psychiatry. 1996; 53:117–128. [PubMed: 8629887]

Miner LH, Jedema HP, Moore FW, Blakely RD, Grace AA, Sesack SR. Chronic stress increases the plasmalemmal distribution of the norepinephrine transporter and the coexpression of tyrosine hydroxylase in norepinephrine axons in the prefrontal cortex. J Neurosci. 2006; 26:1571–1578. [PubMed: 16452680]

Miner LH, Schroeter S, Blakely RD, Sesack SR. Ultrastructural localization of the norepinephrine transporter in superficial and deep layers of the rat prelimbic prefrontal cortex and its spatial

relationship to probable dopamine terminals. J Comp Neurol. 2003; 466:478–494. [PubMed: 14566944]

Muller-Vahl KR, Emrich HM. Cannabis and schizophrenia: towards a cannabinoid hypothesis of schizophrenia. Exp Rev Neurother. 2008; 8:1037–1048.

Muntoni AL, Pillolla G, Melis M, Perra S, Gessa GL, Pistis M. Cannabinoids modulate spontaneous neuronal activity and evoked inhibition of locus coeruleus noradrenergic neurons. Eur J Neurosci. 2006; 23:2385–2394. [PubMed: 16706846]

Nakamoto KT, Mellott JG, Killius J, Storey-Workley ME, Sowick CS, Schofield BR. Analysis of excitatory synapses in the guinea pig inferior colliculus: a study using electron microscopy and GABA immunocytochemistry. Neuroscience. 2013; 237:170–183. [PubMed: 23395860]

Nyilas R, Gregg LC, Mackie K, Watanabe M, Zimmer A, Hohmann AG, Katona I. Molecular architecture of endocannabinoid signaling at nociceptive synapses mediating analgesia. Eur J Neurosci. 2009; 29:1964–1978. [PubMed: 19453631]

Oksanen KM, Waldum ER, McDaniel MA, Braver TS. Neural mechanisms of time-based prospective memory: evidence for transient monitoring. PLoS One. 2014; 9:e92123. [PubMed: 24643226]

Omelchenko N, Sesack SR. Ultrastructural analysis of local collaterals of rat ventral tegmental area neurons: GABA phenotype and synapses onto dopamine and GABA cells. Synapse. 2009; 63:895–906. [PubMed: 19582784]

Oropeza VC, Mackie K, Van Bockstaele EJ. Cannabinoid receptors are localized to noradrenergic axon terminals in the rat frontal cortex. Brain Res. 2007; 1127:36–44. [PubMed: 17113043]

Oropeza VC, Page ME, Van Bockstaele EJ. Systemic administration of WIN 55,212-2 increases norepinephrine release in the rat frontal cortex. Brain Res. 2005; 1046:45–54. [PubMed: 15927549]

Ortega JE, Gonzalez-Lira V, Horrillo I, Herrera-Marschitz M, Callado LF, Meana JJ. Additive effect of rimonabant and citalopram on extracellular serotonin levels monitored with in vivo microdialysis in rat brain. Eur J Pharmacol. 2013; 709:13–19. [PubMed: 23562616]

Page ME, Oropeza VC, Sparks SE, Qian Y, Menko AS, Van Bockstaele EJ. Repeated cannabinoid administration increases indices of noradrenergic activity in rats. Pharmacol Biochem Behav. 2007; 86:162–168. [PubMed: 17275893]

Page ME, Oropeza VC, Van Bockstaele EJ. Local administration of a cannabinoid agonist alters norepinephrine efflux in the rat frontal cortex. Neurosci Lett. 2008; 431:1–5. [PubMed: 18055114]

Parolaro D, Realini N, Vigano D, Guidali C, Rubino T. The endocannabinoid system and psychiatric disorders. Exp Neurol. 2010; 224:3–14. [PubMed: 20353783]

Pavon FJ, Araos P, Pastor A, Calado M, Pedraz M, Campos-Cloute R, Ruiz JJ, Serrano A, Blanco E, Rivera P, Suarez J, Romero-Cuevas M, Pujadas M, Vergara-Moragues E, Gornemann I, Torrens M, de la Torre R, Rodriguez de Fonseca F. Evaluation of plasma-free endocannabinoids and their congeners in abstinent cocaine addicts seeking outpatient treatment: impact of psychiatric co-morbidity. Addict Biol. 2013; 18:955–969. [PubMed: 24283982]

Paxinos, G.; Watson, C. The rat brain in stereotaxic coordinates. Academic Press; Orlando, FL: 1997.

Peters A, Palay SL. The morphology of synapses. J Neurocytol. 1996; 25:687–700. [PubMed: 9023718]

Peters, A.; Palay, SL.; Webster, Hd. The Fine Structure of the Nervous System. Oxford University Press; New York: 1991.

Piomelli D. The molecular logic of endocannabinoid signalling. Nat Rev Neurosci. 2003; 4:873–884. [PubMed: 14595399]

Pistis M, Ferraro L, Pira L, Flore G, Tanganelli S, Gessa GL, Devoto P. Delta(9)-tetrahydrocannabinol decreases extracellular GABA and increases extracellular glutamate and dopamine levels in the rat prefrontal cortex: an in vivo microdialysis study. Brain Res. 2002; 948:155–158. [PubMed: 12383968]

Ramirez-Franco J, Bartolome-Martin D, Alonso B, Torres M, Sanchez-Prieto J. Cannabinoid type 1 receptors transiently silence glutamatergic nerve terminals of cultured cerebellar granule cells. PLoS One. 2014; 9:e88594. [PubMed: 24533119]

Ranganathan M, D'Souza DC. The acute effects of cannabinoids on memory in humans: a review. Psychopharmacology (Berl). 2006; 188:425–444. [PubMed: 17019571]

Reguero L, Puente N, Elezgarai I, Mendizabal-Zubiaga J, Canduela MJ, Buceta I, Ramos A, Suarez J, Rodriguez de Fonseca F, Marsicano G, Grandes P. GABAergic and cortical and subcortical glutamatergic axon terminals contain CB1 cannabinoid receptors in the ventromedial nucleus of the hypothalamus. PLoS One. 2011; 6:e26167. [PubMed: 22022550]

Reyes BAS, Carvalho AF, Vakharia K, Van Bockstaele EJ. Amygdalar peptidergic circuits regulating noradrenergic locus coeruleus neurons: linking limbic and arousal centers. Exp Neurol. 2011; 230:96–105. [PubMed: 21515261]

Reyes BAS, Glaser JD, Magtoto R, Van Bockstaele EJ. Pro-opiomelanocortin colocalizes with corticotropin- releasing factor in axon terminals of the noradrenergic nucleus locus coeruleus. Eur J Neurosci. 2006; 23:2067–2077. [PubMed: 16630054]

Reyes BAS, Johnson AD, Glaser JD, Commons KG, Van Bockstaele EJ. Dynorphin-containing axons directly innervate noradrenergic neurons in the rat nucleus locus coeruleus. Neuroscience. 2007; 145:1077–1086. [PubMed: 17289275]

Reyes BAS, Szot P, Sikkema C, Cathel AM, Kirby LG, Van Bockstaele EJ. Stress-induced sensitization of cortical adrenergic receptors following a history of cannabinoid exposure. Exp Neurol. 2012a; 236:327–335. [PubMed: 22677142]

Reyes BAS, Vakharia K, Ferraro TN, Levenson R, Berrettini WH, Van Bockstaele EJ. Opiate agonist-induced re-distribution of Wntless, a mu-opioid receptor interacting protein, in rat striatal neurons. Exp Neurol. 2012b; 233:205–213. [PubMed: 22001156]

Richter H, Teixeira FM, Ferreira SG, Kittel A, Kofalvi A, Sperlagh B. Presynaptic alpha(2)-adrenoceptors control the inhibitory action of presynaptic CB(1) cannabinoid receptors on prefrontocortical norepinephrine release in the rat. Neuropharmacology. 2012; 63:784–797. [PubMed: 22722024]

Romero-Zerbo SY, Bermudez-Silva FJ. Cannabinoids, eating behaviour, and energy homeostasis. Drug Test Anal. 2014; 6:52–58. [PubMed: 24375977]

Sands SA, Strong R, Corbitt J, Morilak DA. Effects of acute restraint stress on tyrosine hydroxylase mRNA expression in locus coeruleus of Wistar and Wistar-Kyoto rats. Brain Res Mol Brain Res. 2000; 75:1–7. [PubMed: 10648882]

Sawaki K, Baum BJ, Ambudkar IS. Alpha 1-adrenergic and m3-muscarinic receptor stimulation of phosphatidylinositol 4,5-bisphosphate-specific phospholipase C are independently mediated by G alpha q/11 in rat parotid gland membranes. Arch Biochem Biophys. 1995; 316:535–540. [PubMed: 7840663]

Scavone JL, Mackie K, Van Bockstaele EJ. Characterization of cannabinoid-1 receptors in the locus coeruleus: relationship with mu-opioid receptors. Brain Res. 2010; 1312:18–31. [PubMed: 19931229]

Schroeter S, Apparsundaram S, Wiley RG, Miner LH, Sesack SR, Blakely RD. Immunolocalization of the cocaine- and antidepressant-sensitive l-norepinephrine transporter. J Comp Neurol. 2000; 420:211–232. [PubMed: 10753308]

Stella N, Schweitzer P, Piomelli D. A second endogenous cannabinoid that modulates long-term potentiation. Nature. 1997; 388:773–778. [PubMed: 9285589]

Suarez J, Bermudez-Silva FJ, Mackie K, Ledent C, Zimmer A, Cravatt BF, de Fonseca FR. Immunohistochemical description of the endogenous cannabinoid system in the rat cerebellum and functionally related nuclei. J Comp Neurol. 2008; 509:400–421. [PubMed: 18521853]

Sugiura T, Kondo S, Sukagawa A, Nakane S, Shinoda A, Itoh K, Yamashita A, Waku K. 2-Arachidonoylglycerol: a possible endogenous cannabinoid receptor ligand in brain. Biochem Biophys Res Commun. 1995; 215:89–97. [PubMed: 7575630]

Tanimura A, Yamazaki M, Hashimotodani Y, Uchigashima M, Kawata S, Abe M, Kita Y, Hashimoto K, Shimizu T, Watanabe M, Sakimura K, Kano M. The endocannabinoid 2-arachidonoylglycerol produced by diacylglycerol lipase alpha mediates retrograde suppression of synaptic transmission. Neuron. 2010; 65:320–327. [PubMed: 20159446]

Tawfeek HA, Abou-Samra AB. Negative regulation of parathyroid hormone (PTH)-activated phospholipase C by PTH/PTH-related peptide receptor phosphorylation and protein kinase A. Endocrinology. 2008; 149:4016–4023. [PubMed: 18450967]

Trettel J, Levine ES. Cannabinoids depress inhibitory synaptic inputs received by layer 2/3 pyramidal neurons of the neocortex. J Neurophysiol. 2002; 88:534–539. [PubMed: 12091577]

Tsou K, Brown S, Sanudo-Pena MC, Mackie K, Walker JM. Immunohistochemical distribution of cannabinoid CB1 receptors in the rat central nervous system. Neuroscience. 1998; 83:393–411. [PubMed: 9460749]

Turu G, Hunyady L. Signal transduction of the CB1 cannabinoid receptor. J Mol Endocrinol. 2010; 44:75–85. [PubMed: 19620237]

Tzavara ET, Davis RJ, Perry KW, Li X, Salhoff C, Bymaster FP, Witkin JM, Nomikos GG. The CB1 receptor antagonist SR141716A selectively increases monoaminergic neurotransmission in the medial prefrontal cortex: implications for therapeutic actions. Br J Pharmacol. 2003; 138:544–553. [PubMed: 12598408]

Tzavara ET, Perry KW, Rodriguez DE, Bymaster FP, Nomikos GG. The cannabinoid CB(1) receptor antagonist SR141716A increases norepinephrine outflow in the rat anterior hypothalamus. Eur J Pharmacol. 2001; 426:R3–4. [PubMed: 11527547]

Uchigashima M, Narushima M, Fukaya M, Katona I, Kano M, Watanabe M. Subcellular arrangement of molecules for 2-arachidonoyl-glycerol-mediated retrograde signaling and its physiological contribution to synaptic modulation in the striatum. J Neurosci. 2007; 27:3663–3676. [PubMed: 17409230]

Van Bockstaele EJ, Chan J, Pickel VM. Input from central nucleus of the amygdala efferents to pericoerulear dendrites, some of which contain tyrosine hydroxylase immunoreactivity. J Neurosci Res. 1996a; 45:289–302. [PubMed: 8841990]

Van Bockstaele EJ, Colago EE, Valentino RJ. Corticotropin-releasing factor-containing axon terminals synapse onto catecholamine dendrites and may presynaptically modulate other afferents in the rostral pole of the nucleus locus coeruleus in the rat brain. J Comp Neurol. 1996b; 364:523–534. [PubMed: 8820881]

Wager-Miller J, Westenbroek R, Mackie K. Dimerization of G protein-coupled receptors: CB1 cannabinoid receptors as an example. Chemistry and physics of lipids. 2002; 121:83–89. [PubMed: 12505693]

Wang H, Lupica CR. Release of endogenous cannabinoids from ventral tegmental area dopamine neurons and the modulation of synaptic processes. Prog Neuropsychopharmacol Biol Psychiatry. 2014; 52:24–27. [PubMed: 24495779]

Wang Z, Li JY, Dahlstrom A, Danscher G. Zinc-enriched GABAergic terminals in mouse spinal cord. Brain Res. 2001; 921:165–172. [PubMed: 11720723]

Yoshida T, Uchigashima M, Yamasaki M, Katona I, Yamazaki M, Sakimura K, Kano M, Yoshioka M, Watanabe M. Unique inhibitory synapse with particularly rich endocannabinoid signaling machinery on pyramidal neurons in basal amygdaloid nucleus. Proc Natl Acad Sci U S A. 2011; 108:3059–3064. [PubMed: 21282604]

Yu H, Seo JB, Jung SR, Koh DS, Hille B. Noradrenaline upregulates T-type calcium channels in rat pinealocytes. J Physiol. 2015; 593:887–904. [PubMed: 25504572]

Zamberletti E, Beggiato S, Steardo L Jr, Prini P, Antonelli T, Ferraro L, Rubino T, Parolaro D. Alterations of prefrontal cortex GABAergic transmission in the complex psychotic-like phenotype induced by adolescent delta-9-tetrahydrocannabinol exposure in rats. Neurobiol Dis. 2014; 63:35–47. [PubMed: 24200867]

Zander JF, Munster-Wandowski A, Brunk I, Pahner I, Gomez-Lira G, Heinemann U, Gutierrez R, Laube G, Ahnert-Hilger G. Synaptic and vesicular coexistence of VGLUT and VGAT in selected excitatory and inhibitory synapses. J Neurosci. 2010; 30:7634–7645. [PubMed: 20519538]

Zhang J, Muller JF, McDonald AJ. Noradrenergic innervation of pyramidal cells in the rat basolateral amygdala. Neuroscience. 2013; 228:395–408. [PubMed: 23103792]

Highlights

- NET or DβH-containing fibers are in close apposition with DGL-α-immunoreactive (IR) neurons in FC
- NET or DβH-axon terminal are directly apposed to DGL-α-IR neurons in FC at ultrastructural level
- CB1r and DβH were co-localized in fibers that were closely apposed with DGL-α

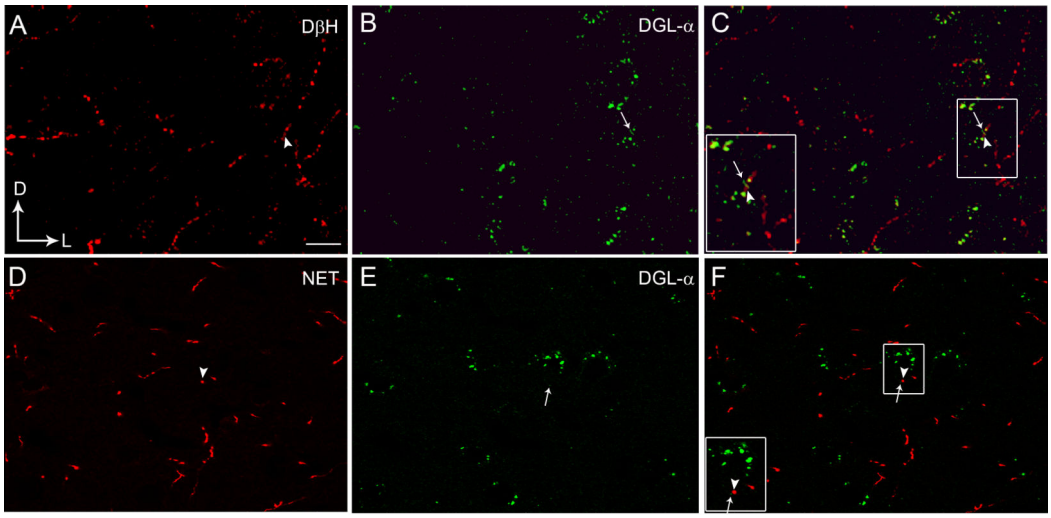

Figure 1.

Confocal fluorescence photomicrographs showing immunolabeling of diacylglycerol lipase-α (DGL-α) in the frontal cortex with respect to noradrenergic afferents as visualized by the presence of dopamine-β-hydroxylase (DβH) or the norepinephrine transporter (NET) (Panels **A-F**). **A.** DβH was detected using a rhodamine isothiocyanate-conjugated secondary antibody (TRITC donkey anti-mouse; red). **B.** DGL-α was detected using a fluorescein isothiocyanate-conjugated secondary antibody (FITC donkey anti-rabbit; green). **C.** Merged image of panels A and B. The inset shows a higher magnification view of the area outlined by the boxed region showing close associations between DβH (arrowhead) and DGL-α (arrow). **D**. NET (red) was detected using a TRITC donkey anti-mouse secondary antibody. **E**. DGL-α (green) was detected using a FITC donkey anti-rabbit secondary antibody. **F.** Merged image of panels D and E. The inset shows a higher magnification view of the area outlined by the boxed region showing close associations of NET (arrowhead) with DGL-α (arrow). Scale bars = 100 μm.

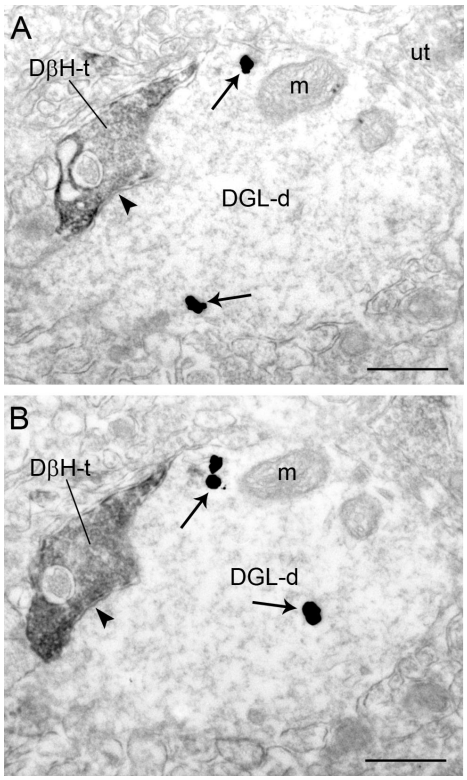

Figure 2.

Electron micrographs showing immunoperoxidase labeling for dopamine-β-hydroxylase (DβH) in an axon terminal and immunogold-silver labeling for diacylglycerol lipase-α (DGL-α) in a dendrite in the frontal cortex. **A-B.** Adjacent sections depicting a DβH-t that forms a symmetric synapse (arrowheads) with a DGL-d. Arrows point to immunogold-silver labeling. m: mitochondria; ut: unlabeled terminal. Scale bars = 0.50 μm.

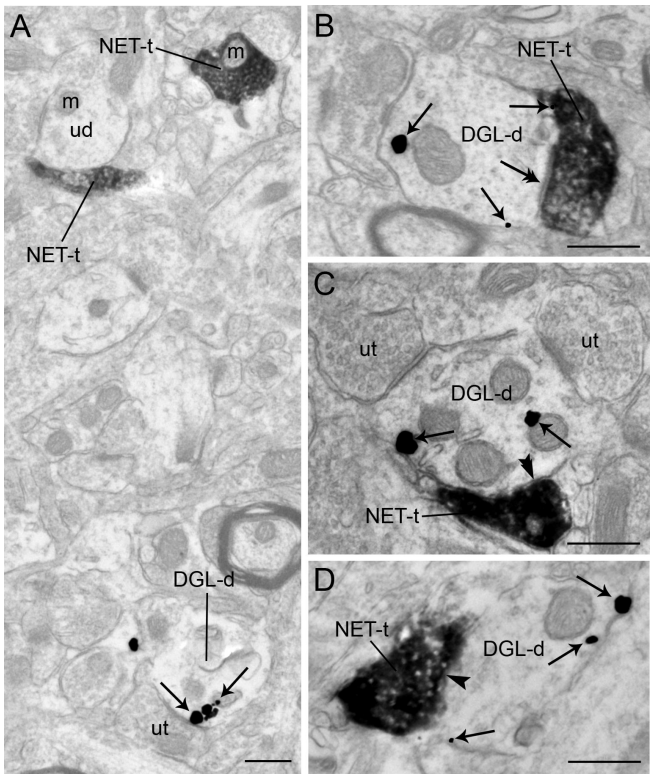

Figure 3.

Electron micrographs showing immunoperoxidase labeling for the norepinephrine transporter (NET) in axon terminals and immunogold-silver labeling for diacylglycerol lipase-α (DGL-α) in dendrites in the the frontal cortex. **A.** Two NET-labeled axon terminals (NET-t) are shown in the same field as a DGL-α-labeled dendrite (DGL-d). **B.** Immunoperoxidase labeling can be seen in a NET-immunoreactive axon terminal (NET-t) contacting (double arrows) a DGL-d. **C.** Dense immunoperoxidase labeling can be seen in a NET-t that forms a symmetric synapse (double arrowheads) with a DGL-d. Also shown are two unlabeled axon terminals (ut) that form a contact with the same DGL-d. **D.** A dense NET-t contacts (arrowhead) a DGL-d. Black arrows point to immunogold-silver labeling for DGL-α throughout. m: mitochondria; ut: unlabeled terminal. Scale bars = 0.50 μm

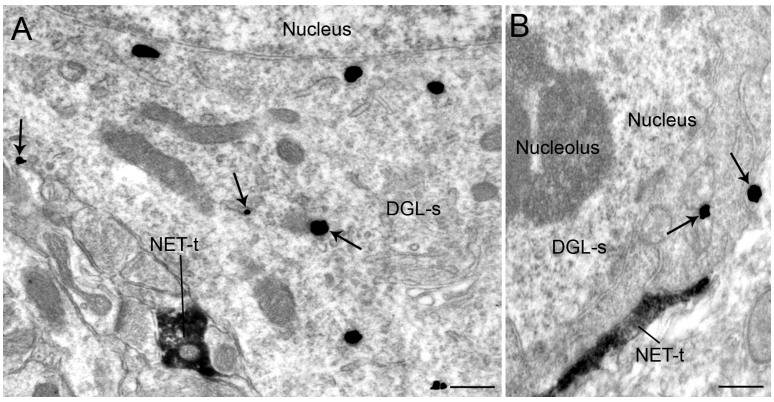

Figure 4.

Electron micrographs showing immunoperoxidase labeling for the norepinephrine transporter (NET) in axon terminals and immunogold-silver labeling for diacylglycerol lipase-α (DGL-α) in the frontal cortex (FC). **A-B.** NET-labeled axon terminals (NET-t) are directly contacting perikarya containing immunogold silver labeling for DGL-α (DGL-s). Arrows point to immunogold-silver labeling. Scale bar, 0.50 μm.

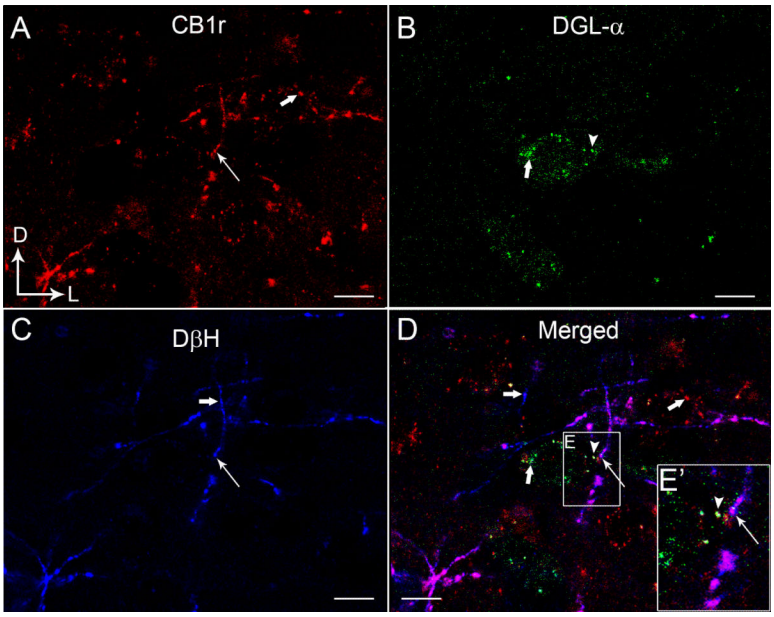

Figure 5.

Confocal fluorescence micrographs showing cannabinoid receptor type 1 (CB1r, **A**), 1,2 diacylglycerol lipase-α (DGL-α, **B**) and dopamine-β-hydroxylase (DβH, **C**) in the rat frontal cortex (FC). CB1r was detected using a rhodamine isothiocyanate-conjugated secondary antibody (TRITC donkey anti-guinea pig; red) and DGL-α was detected using a fluorescein isothiocyanate-conjugated secondary antibody (FITC-donkey anti-rabbit; green). DβH-labeling was detected using Cy5 donkey anti-mouse secondary antibody (blue). CB1r and DβH appeared punctate throughout. The merged image (**D**) shows co-localization of CB1r and DβH in the same processes (white thin arrows) and in close proximity to DGL-α (arrowhead) in the FC. Thick white arrows indicate single-labeling (CB1r, DGL or DβH). The inset shows a higher magnification view of the area outlined by the boxed region showing close associations between DβH/CB1r and DGL-α. Scale bars, 100 μm.

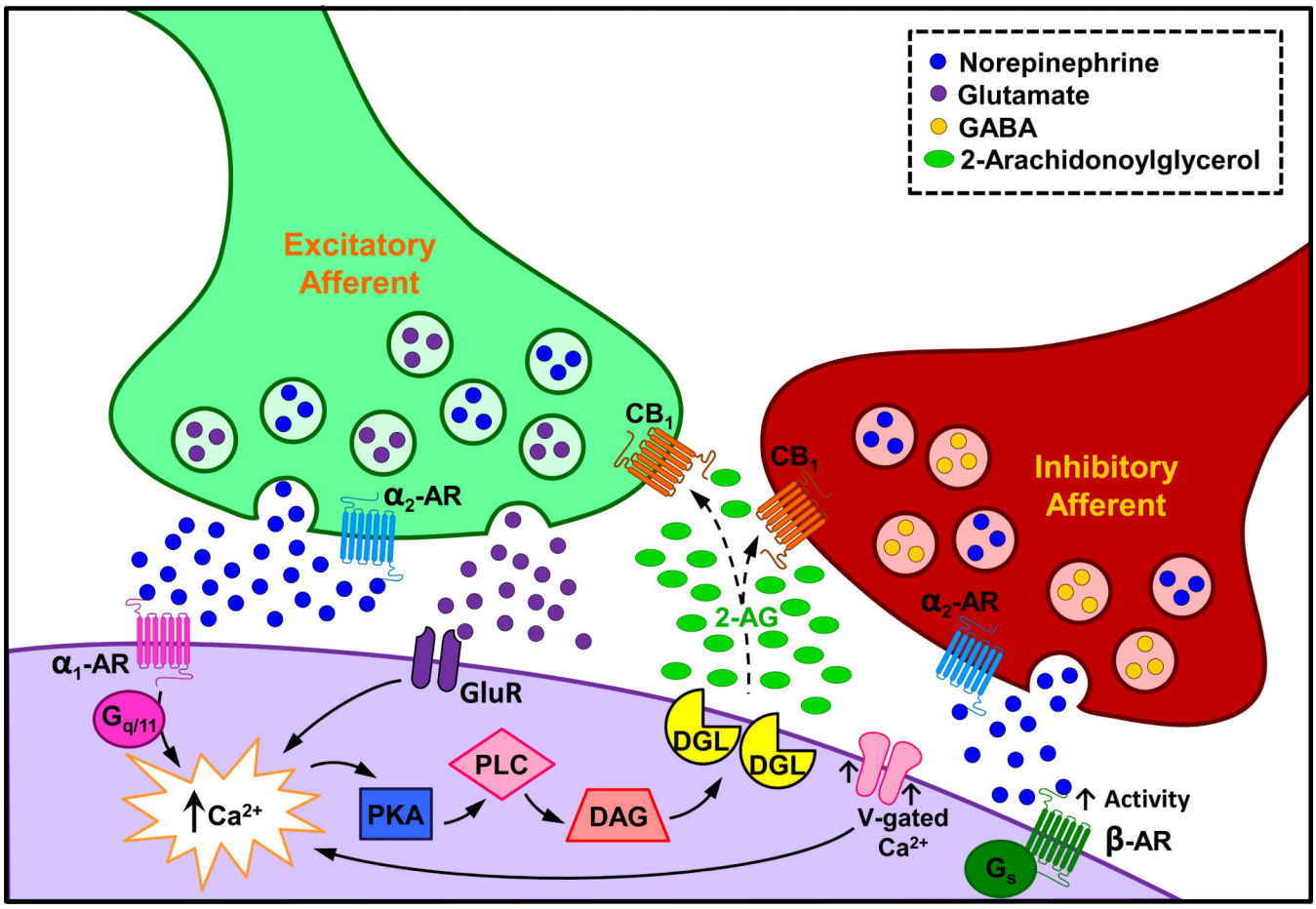

Figure 6.

Schematic diagram depicting proposed mechanisms underlying modulation of NE afferents by the eCB system. Noradrenergic axon terminals that express CB1r may co-localize inhibitory transmitters, such as gamma-amino butyric acid (Hajos *et al.*, 2000; Ranganathan and D'Souza, 2006), or may co-localize excitatory transmitters such as glutamate (Katona *et al.*, 2006; Kawamura *et al.*, 2006). Excitatory ionotropic or G protein-coupled receptor activation (via excitatory amino acid, alpha1 or beta-adrenergic receptors), stimulate calcium production and engage intracellular pathways that contribute to local eCB synthesis and release. Following activation, 2-AG may diffuse into the synapse and bind to CB1r located on noradrenergic terminals that co-express inhibitory or excitatory transmitters. Functional consequences of eCB modulation of cortical afferents include inhibition of inhibitory neurotransmitter release as cannabinoids have been shown to reduce inhibitory neurotransmitter efflux (Trettel and Levine, 2002; Zamberletti *et al.*, 2014) and increased excitatory neurotransmitter release (Galanopoulos *et al.*, 2011). Once NE is released, the possibility exists that it could bind to pre-synaptically distributed alpha2 adrenergic receptors that are coupled to inhibitory Gi proteins, and through their activation, further tonically inhibit NE. In addition to alterations in NE, retrograde suppression of inhibitory neurotransmitter release and increases in excitatory neurotransmitter release in FC may affect synaptic integration and cortical neuronal activity. Furthermore, it is also feasible that NE activates the beta adrenergic receptor thereby increasing neuronal activity by activation

of voltage-gated calcium channels (Yu et al., 2015) thereby increasing calcium influx resulting in neuronal depolarization and consequently increased 2-AG production.